University of Nebraska - Lincoln

DigitalCommons@University of Nebraska - Lincoln

Mechanical & Materials Engineering Faculty Publications

Mechanical & Materials Engineering, Department of

2016

A Comparative Study on Machining Capabilities of Wet and Dry Nanoscale Electro-machining

Muhammad P. Jahan
Western Kentucky University, muhammad.jahan@wku.edu

Kamlakar P. Rajurkar
University of Nebraska-Lincoln, krajurkar1@unl.edu

Ajay P. Malshe
University of Arkansas, Fayetteville

Follow this and additional works at: http://digitalcommons.unl.edu/mechengfacpub

Part of the Mechanics of Materials Commons, Nanoscience and Nanotechnology Commons, Other Engineering Science and Materials Commons, and the Other Mechanical Engineering Commons

18th CIRP Conference on Electro Physical and Chemical Machining (ISEM XVIII)

A Comparative Study on Machining Capabilities of Wet and Dry Nano-scale Electro-machining

Muhammad P. Jahan[a],*, Kamlakar P. Rajurkar[b], Ajay P. Malshe[c]

aArchitectural and Manufacturing Sciences Department, Western Kentucky University, Bowling Green, KY 42101, USA
bDepartment of Mechanical and Materials Engineering, University of Nebraska, Lincoln, NE 68588, USA
cDepartment of Mechanical Engineering, University of Arkansas, Fayetteville, AR 72701, USA

* Corresponding author. Tel.: +1-270-745-2176; fax: +1-270-745-5946. *E-mail address:* muhammad.jahan@wku.edu

Abstract

Presently, the nano scale electro-machining (nano-EM) process has been demonstrated in both the liquid and air dielectric mediums, which are known as wet and dry nano-EM respectively. In the current study, two important aspects of the nano-EM have been investigated: the minimum possible feature dimension and mass fabrication capability of nano-EM. Firstly, the investigation has been done on the capability of machining graphene at atomic scale with focus on obtaining smallest possible nano-feature using the wet nano-EM. Secondly, the ability of the nano-EM process for the fabrication of arrays of nano-holes has been investigated using dry nano-EM. It was found that nano-features of 3 to 4 nm could be machined in graphene surfaces revealing the atomic arrangement of carbon using the wet nano-EM process. The dry nano-EM was found to be capable of fabricating arrays of nano-features making it more suitable for mass fabrication. The field induced evaporation of materials from the tool during dry nano-EM retained the quality of tool electrode, thus making the process capable of fabricating more than 100 nano features in a single step. It was found that the material removal mechanism influenced the machining capability of the process. The mechanism of material removal in the wet nano-EM was associated with the dielectric breakdown of liquid n-decane generating intense heat for ionization, evaporation, and melting of materials. On the other hand, the material removal mechanism of dry nano-EM was associated with the breakdown of air, which generated intense heat at the gap between the nano-EM tool and the workpiece causing localized ionization and evaporation.

1. Introduction

In recent years, a significant number of nano-structures are used for different important applications in electronics, nano-electro-mechanical systems (NEMS) and biomedical components. Some of the driving applications of different nano-features are: nano-pores for DNA detection devices, nano-vias for interconnects, nano-jets for controlled drug release, next generation fuel atomizers, nozzles for nano-fluidic devices, molecular sieves for protein sorting and so on [1-4]. In order to meet the increasing demand of nano-structures, a number of nanofabrication techniques have been developed, such as photolithography [5], nano imprint lithography [6], focused ion beam lithography [7], UV lithography [8], X-ray lithography [8], electron beam lithography [9], soft lithography [10], edge lithography [11], femtosecond laser machining [12], SPM based lithography [13] and so on. Although most of these nanofabrication techniques addressed material removal from silicon and polymeric materials [14], very few of them have addressed machining of conducting but hard surfaces. The fabrication of nanoscale features in different functional metals like gold, nickel, copper, titanium alloys are of prime importance for different electronic and biomedical applications [15]. In addition, many of the lithography processes are limited by the minimum achievable feature size and process contamination [16]. A comparative performance of different nanomanufacturing techniques with respect to minimum

feature size, contamination possibility, processing speed, scalability and cost has been presented elsewhere [17].

Among the unconventional techniques of nanofabrication, SPM has emerged to be a unique tool for materials structuring and patterning with atomic and molecular resolution [18]. The most important benefit of SPM based lithography is that it has extreme site-specificity and locality, and can be operated in a variety of media such as vacuum, air and fluids [19]. A number of studies have been conducted on the STM lithography in ultrahigh vacuum [20]. In addition, research has been conducted on STM lithography under the presence of aqueous environment using water and ethanol vapor [21]. Several mechanism of material removal or deposition have been proposed, such as field induced diffusion, material transfer, field evaporation, electro-migration and so on [22]. However, many of the studies have reported inconsistency in the both fabrication mechanism and the stability of nano-features, although they used controlled environment.

In order to address the issue of nano-structuring in conducting and difficult-to-cut materials and improve consistency and stability of nano-features, a nano-electro-machining process based on scanning tunneling microscope (STM) platform has been developed by the co-authors [14]. The operational capability of STM in vacuum, air and liquid media has contributed to the development of nano-EM processes in both liquid medium (wet nano-EM) [14] and air medium (dry nano-EM) [23]. In the nano-EM process, Platinum-Iridium [Pt-Ir (80:20)] or Tungsten [99.9%W] is used as tool electrode and any conducting substrates with atomic level surface roughness is used as workpiece. For the dielectric, liquid n-decane is used in wet nano-EM and air is used in dry nano-EM. Several research studies have been carried out on the wet and dry nano-EM. The previous studies in the area of wet nano-EM focused on the feasibility [14], repeatability [16], dielectric breakdown [24], tool wear characteristics [24], dielectric molecular medium [25], and molecular dynamics simulation of the machining interface [25]. Moreover, the feasibility, mechanism and machining performance of dry nano-EM have been discussed [23]. However, two major research questions for the nano-EM processes are the minimum feature dimension and ability of the process for mass fabrication of nano-features. In this study, two aspects of the nano-EM have been presented. First, investigation has been done on the capability of machining graphene at atomic scale with focus on obtaining smallest possible nano-feature. Wet nano-EM process using n-decane as dielectric has been used for this investigation. Secondly, the ability of the nano-EM process for the fabrication of arrays of nano-holes has been investigated using dry nano-EM. The reason for choosing dry nano-EM for mass fabrication is its ability to retain the tip quality for long period [23].

2. Experimental detail

A Digital Instruments (DI) Multimode Scanning Tunneling Microscopy (STM) with NanoScope IV controller is modified to perform the dry and wet nano-EM as shown in Fig. 1. An atomically sharp conducting tip/probe is brought within a few atom diameters (≈ 1 nm) of the conducting surface that needs to be machined. A bias voltage high enough to cause the breakdown of dielectric fluid at the gap between tool/tip and workpiece is applied for electro-machining. The STM modified setup for nano-electro-machining can be compared to the conventional die-sinking EDM, where the electrode and the workpiece are kept at distance of several microns. The gap between the electrode and workpiece (working gap/spark gap) is filled with either liquid or air dielectric and voltage is applied for the occurrence of electrical discharges, which removes the materials from both the electrode and workpiece.

In this study, the graphene films deposited on the conductive nickel surface were used as the substrate/work piece for wet nano-EM. On the other hand, the hydrogen flame annealed atomically flat {111} gold grown using molecular beam epitaxy (MBE) on mica was used as workpiece for dry nano-EM. The Pt-Ir (80:20) was used as tool electrode due to its stable performance and ability of retaining tip quality for the long period. The tools have been fabricated by electrochemical etching process. The quality of the nano-EM tools have been evaluated in-situ before and after the machining using the method developed by the authors [23]. In case of wet nano-EM, n-decane was used as dielectric liquid, whereas for dry nano-EM, no additional dielectric material was used at the gap between the tip and substrate, considering atmospheric air as a dielectric medium. The machining conditions for wet and dry nano-EM are listed in table 1. The dry and wet nano-EM was conducted in near field in a constant current mode.
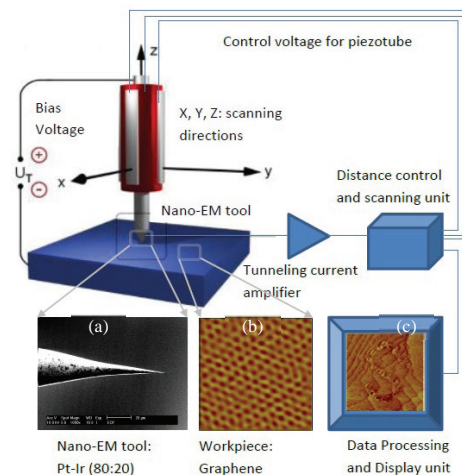

Fig. 1. Schematic representation of the nano-EM setup; (a) SEM image of atomically sharp Pt-Ir (80:20) tip, (b) atomic resolution the STM image of the graphene surface, and (c) machining of letter "S" on graphene as shown in the display unit after machining by nano-EM.

Table 1. Machining Conditions for wet and dry nano-EM

Machining platform	STM
Work piece	Graphene
Tool/tip	Pt-Ir (80:20)
Dielectric	n-decane (wet nano-EM), air (dry nano-EM)
Machining voltage	2,600 – 3,600 mV
Machining current	1 nA
Pulse duration	1 – 5 sec per nano-feature

3. Machining of smallest possible nano-feature in graphene using wet nano-EM

In this section, the investigation for obtaining smallest possible nano-hole in graphene has been presented. Fig. 2(a) shows the atomic resolution image of the graphene in n-decane dielectric medium. A bias voltage of 200 mV and tunneling current of 1 nA were used for obtaining atomic resolution image of graphene. The lattice parameter measured from the atomic resolution image was found to be 2.4 ±0.2Å, which is comparable to the theoretical value of 2.46Å [26]. For the machining of graphene at atomic scale it was assured that the atomic arrangement were seen in the image of machined feature. It was found that the 10 nm x 10 nm was the largest scan size where the atomic arrangement of carbons in graphene could be realized clearly [Fig. 1(b)]. For machining graphene at atomic scale, the bias voltage and the pulse duration were optimized by trial and error. It was found that positive bias voltage ranging from 2600 mV – 3500 mV provided consistent nano-features.
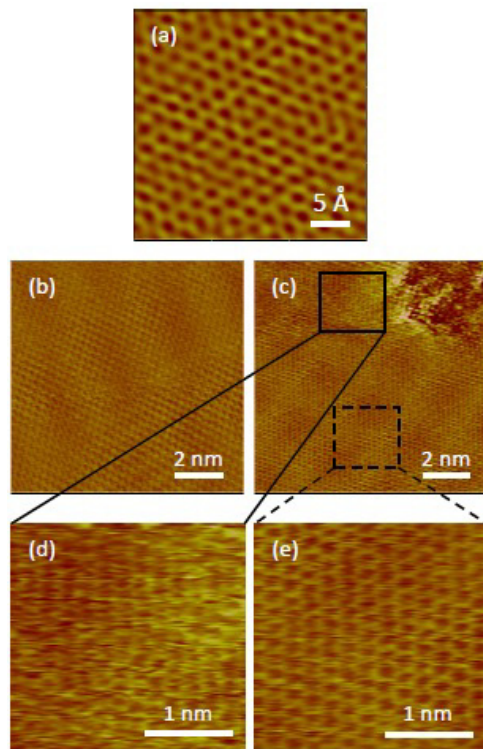

Fig. 2. (a) Atomic resolution STM image of graphene (3 nm x 3 nm, 200 mV, 1nA), (b) Current image (constant-height) of 10 nm x 10 nm graphene surface before machining (200 mV, 1nA), (c) Current image of the same 10 nm x 10 nm graphene surface after machining (at 2600 mV, 1 nA, 3 sec), (d) Magnified image taken adjacent to the machined nano-hole, (e) Magnified image taken from un-machined area.

The negative bias voltage was found unsuitable for machining of features in graphene, showing rather deposition of materials on the graphene surface. Using bias voltage more than 3200 mV resulted in bigger heat affected zone (HAZ) in

the workpiece as well as damaged the nano-EM tool seriously. The nano-EM tool quality was monitored *in-situ* both before and after machining each hole by $I – Z$ curves. The most important parameter was found to be the pulse duration. It was observed that the machining of graphene required longer duration of voltage pulse. The pulse duration below 3 sec was found to provide inconsistent features, although the bias voltage was increased. This might be due to the higher elasticity of graphene resulting from higher bonding strength of carbon atoms [27]. The threshold energy for carbon atom displacement from the lattice was found to be very high [18 to 22 eV] [27]. Fig. 2(b) and (c) shows the graphene surface before and after machining by the nano-EM process. The entire hole was not covered in Fig. 2(c), which was taken immediately after machining, due to the drift of the STM tip. Considering the hole as a quarter of nano-hole [see Fig. 3(c) also], the hole-radius was measured as 1.758 nm with the depth of 0.206 nm. From the measured depth, it can be said that the machining was carried out on a single layer of graphene, as the thickness of monolayer graphene is 0.335 nm [26]. Fig. 2(d) reveals that the lattice structure of graphene around the edge of the nano-hole was clearly affected after machining. This may be due to the fact that the graphene lattice went into structural disorder and amorphization upon the application of electrical energy [28]. There was partial reconstruction of the lattice structure and evaporation of carbon atoms from these HAZ over the time [29].
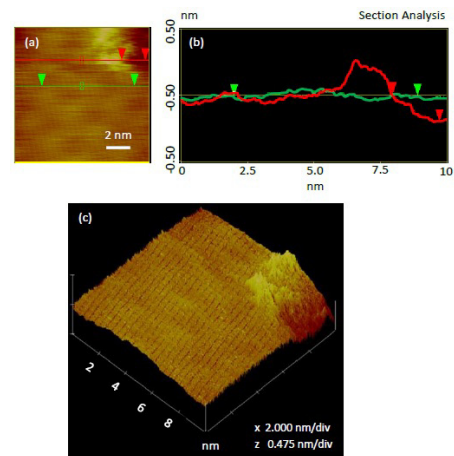

Fig. 3. (a) Height (constant-current) image of Figure 6(c) showing the deposited materials at the edge of the hole [hole radius 1.758 nm, depth 0.206 nm], (b) Section analysis showing the profile of the machined hole and, (c) 3D image showing the quarter of a nano-hole.

Despite reconstruction of graphene lattice there was still deposition of materials at the edge of the nano-hole [Fig. 3(a), (c)]. This may be due to the higher energy required to evaporate carbon atom from the reconstructed edges [29]. The energy required for removal of single carbon atom from a reconstructed pentagon – heptagon (5-6) pair was found to be 10.6 eV [29]. As a result, removed carbon atoms from the lattice showed a tendency to accumulate at the edge of the nano-hole. The accumulation of material at the edge of the nano-hole may also be associated with the spontaneous

curling of graphene sheet at the reconstructed edges due to tensile edge stress [30]. The height of the deposited material at the nano-hole edge was nearly equal to the depth of the hole [Fig. 3(b)].
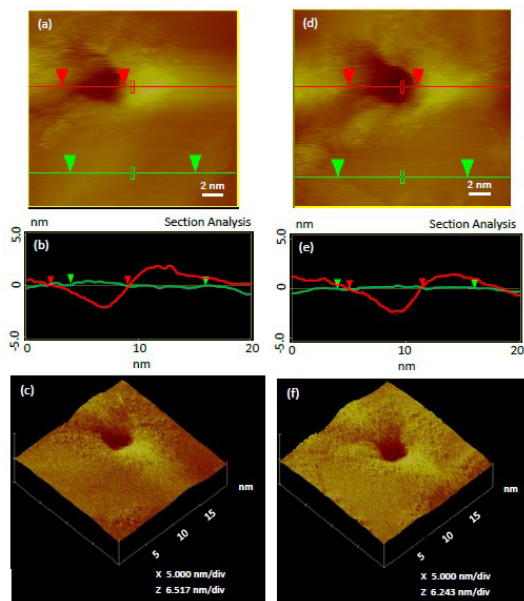

Fig. 4. The 20 nm x 20 nm constant-current image [(a) & (d)], section analyses of nano-holes [(b) & (e)] and 3D image [(c) & (f)] at 2800 mV, 1 nA, 3 sec.

To investigate the consistency in machining behavior of graphene and repeatability of the process, machining was conducted over 20 nm x 20 nm areas under machining condition of 2800 mV bias voltage, 1 nA current, 3 sec pulse duration [Fig. 4]. The diameter and depth of two holes were measured as 5.938 nm and 2.468 nm for hole-1, [Fig. 4(a)-(c)] and 6.406 nm and 3.125 nm for hole-2, [Fig. 4(d)-(e)]. The same phenomenon of recast layer formation at the edge of the nano-holes was observed in both cases. The profiles of the deposited materials were found to be nearly the reverse of the machined hole. In addition, the volume of the deposited materials was measured as 50 – 80% of the removed materials. Therefore, about 20 – 50% of the materials were evaporated from the graphene substrate and rests were deposited around the edge of the nano-holes.

The mechanism of material removal in wet nano-EM of graphene was associated with the dielectric breakdown of liquid n-decane. The selected bias voltage was high enough to create field strength greater than the critical breakdown strength of n-decane. The field strength created by applying the bias voltage of 2600 mV – 3500 mV at the gap of 0.5 – 2 nm created a field strength of higher than 1×10^9 V/m, which was reported to be the breakdown strength of n-decane, and found to be independent of cathode material (nano-EM tool tip) [31]. Upon breakdown of the dielectric, a large amount of current ran through the gap that resulted in the machining of nano-features in graphene. It was reported that a cathode shank diameter of 100 nm could result in current density of

1.3×10^3 A/m² inside the gap upon breakdown of n-decane, which was enough for causing the heating, melting and evaporation of materials [31]. At the end of the applied voltage pulse, the gap recovered its strength as fresh dielectric was drawn into the gap to replace the vapors created in the gap. As the dielectric was stagnant from the macroscopic point of view, the motion of the new dielectric into the gap was mainly associated with the diffusion process for concentration gradient between fresh dielectric and dielectric vapor in gap. The melted portions of the materials might be removed by the flow of dielectric liquid or re-deposited around the edge of the nano-hole.

4. Nano-patterning in gold using dry nano-EM

The dry nano-EM was done using a Pt-Ir (80:20) tool electrode on the atomically flat gold surface in the presence of atmospheric air. Fig. 5 presents the machining of the letter "S" with a series of nano-holes on the gold substrate. It can be observed that, except one or two holes, most of the holes were consistent and well defined. The section analysis across the different nano-features in Fig. 5 suggests that, all the holes were nearly same in dimension and also the depth of the features were nearly same. The diameters of the nano-holes as indicated by red, green and white markers in the section analysis were 10.588, 11.871 and 10.730 nm respectively. The machining depths measured for the holes indicated by red, green and white arrows were 0.821, 0.695 and 0.786 nm respectively. It can be observed from the cross-sectional profile shown in Fig. 5 that all the nano-holes were nearly "V" shaped, indicating that there was definitely machining occurred. If we consider the case of conventional die-sinking EDM or micro-EDM, we know that the negative image of the electrode is formed after machining. Similarly, in case of dry nano-EM, the shape of the machined profile was nearly similar to the negative shape of the STM tip, which confirmed the machining was happened under the presence of air. One important observation is that, although the shapes of the nano-features were negative profile of STM tip, the nano-feature diameter was much lesser than the actual STM tip. It was reported that, the end radius of a quality 1 tip was 30 – 40 nm, with >50 nm for quality 2 and >70 nm for quality 3 tips [23]. However, the average radius of the profiles of the nano-features machined by dry nano-EM was about 4 – 6 nm, which was much smaller than that of a STM tip. This phenomenon clearly proved the non-contact nature of machining, which means there was no direct mechanical contact between the tip and the substrate during dry nano-EM.

The mechanism of dry nano-EM was associated with the breakdown of air, which caused the localized ionization and evaporation, and finally resulted in the material removal. During machining of nano-features, there was a sudden rise in the current due to the application of high bias voltage. During application of very high bias voltage, this sudden rise in the current at gap width resulted in the field induced evaporation of materials from both the gold substrates and the Pt-Ir tip. The field induced evaporation of materials from both the tip and substrate was also suggested by one important finding in this study. During machining, the quality of the tip became

better and sharper, and produced smaller and more consistent nano-features. The improvement in the quality of the tip could easily be explained by the field evaporation principle [23]. During the application of high bias voltage in dry nano-EM, there might be intense local heating at the region of machining. Due to this intense heating, the materials got evaporated from the nano-EM tip, especially from different asperities of the tip, thus making the tip sharper.
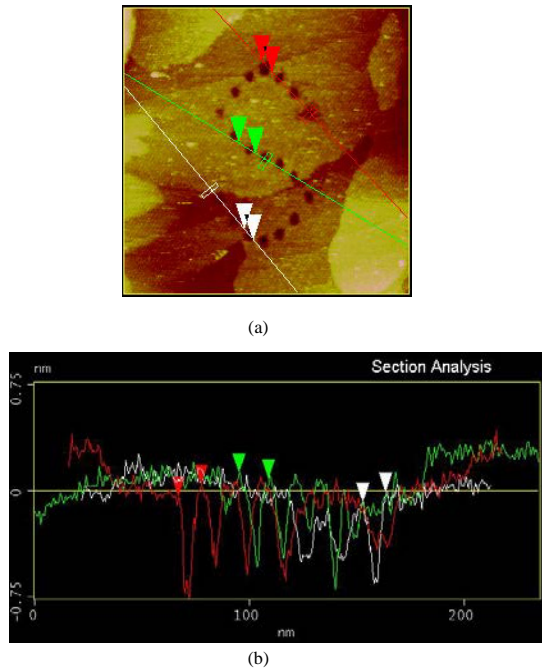

(a)

(b)

Fig. 5. (a) Cross-section across different nano-features obtained using dry nano-EM applying bias voltage of 3200 mV, 1 nA current pulse for 1 second pulse duration per feature, (b) The profiles of different nano-holes obtained across three different lines of cross-section.

Fig. 6(a), (b) and (c) shows the machining of "NSF", "USA" and the 'Map of USA' respectively using arrays of nano-holes with dry nano-EM in a single step. It was found that all the 50 holes in the writing of "NSF" were identical. The average diameter of the 50 nano-holes was measured as 7.5 nm. In case of writing of "USA", it can be seen that except one hole from letter 'A', most of the holes were well defined and of almost same dimensions [Fig. 6(b)]. The dimensions of all the 39 nano-holes were measured and it was found that the average diameter of the holes was closely 10 nm. Fig. 6(c) shows the image of the "Map of USA" that was machined by defined nano-features using dry nano-EM. It was found that some of the nano-holes were not machined properly due to the uneven surface. The nano-holes machined on the smooth surface were almost identical and well defined. One of the major challenges in nanofabrication using dry nano-EM was the roughness of the surface. As mentioned before in the experimental section, the surface roughness should be in the angstrom level in order to ensure all the nano-features are machined properly. Moreover, it was observed that machining of nano-features at the grain boundary of atomically flat gold

atoms did not provide very well defined features, as can be seen from Fig. 6(c). Therefore, selection of proper surface with lesser grain boundaries by continuous scanning is important prior to running the nanoscript for machining.
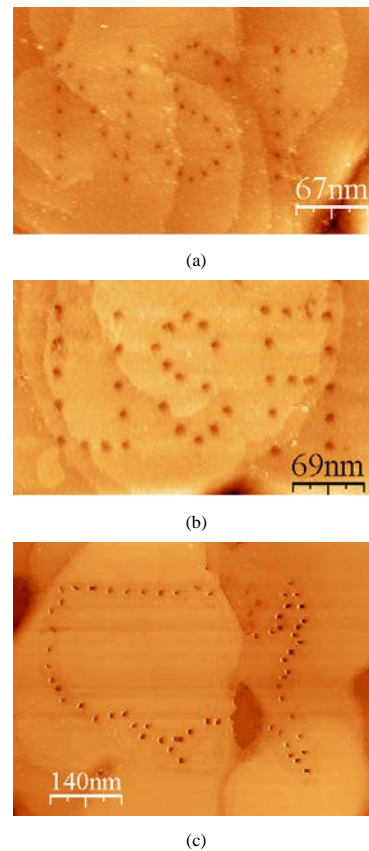

(a)

(b)

(c)

Fig. 6. Nano patterning in gold by mass fabrication of nano-holes in a single step using dry nano-EM: (a) machining of letters "NSF", (b) machining of letters "USA" and (c) machining of the "USA map".

Table 2. Differences between wet nano-EM and dry nano-EM

Factors of comparison	Wet nano-EM	Dry Nano-EM
Machining Platform	STM	STM
Electrode	Pt / Ir, Tungsten	Pt / Ir, Tungsten
Electrode diameter	20-30 nm	20-30 nm
Discharge gap	2-10 nm	2-10 nm
Dielectric medium	n-decane, hydrocarbon oil	Atmospheric air
Electric field strength	1×10^9 V/m	3×10^6 V/m
Material removal Mechanism	Dielectric breakdown of n-decane causes high current intensity resulting in melting and evaporation of materials	Breakdown of air causes intense heat and electric field resulting in field induced evaporation of ions and atoms
Average Feature size	10 mm	7.5 nm
Minimum Feature size	3-5 mm	3-5 nm

As can be seen from the discussions in sections 3 and 4, the differences between the wet and dry nano-EM exist mainly due to the different mediums used for two processes. The differences also exist in the material removal mechanism, electric field strength, and the machining capabilities of the two processes. However, there is no significant difference in the basic experimental setup, electrode and workpiece materials, and the discharge gap between the electrode and workpiece during machining. Table 2 presents a summary of the differences between wet and dry nano-EM considering various aspects of machining.

5. Conclusions

The following conclusions can be drawn from this experimental study:
- The smallest nano-feature of 3 to 4 nm can be machined in 10 nm x 10 nm graphene surfaces showing the atomic arrangement of carbon using the wet nano-EM process in n-decane dielectric interface.
- The mechanism of material removal in the wet nano-EM is associated with the dielectric breakdown of liquid n-decane generating intense heat for ionization, evaporation, and/or melting of materials.
- The material removal mechanism of dry nano-EM is associated with the breakdown of air, which generates intense heat at the gap between the nano-EM tool and the workpiece causing localized ionization and evaporation.
- The field induced evaporation from the tool during dry nano-EM improves the quality of the tool for both scanning and further machining, thus making the dry nano-EM process suitable for mass fabrication of nano-features.
- The dry nano-EM can fabricate arrays of nano-features in a programmed way with very good repeatability and consistency of the features.

References

[1] Li J, Gershow M, Stein D, Brandin E, Golovchenko JA. DNA molecules and configurations in a solid-state nanopore microscope. Nature Materials 2003;2:611-15.

[2] Moseler M, Landman U. Formation, stability, and breakup of nanojets. Science 2000;289:1165-169.

[3] Kresge CT, Leonowicz ME, Roth WJ, Vartuli JC, Beck JS. Ordered mesoporous molecular sieves synthesized by a liquid-crystal template mechanism. Nature 1992;359:710-12.

[4] Xie XN, Chung HJ, Wee ATS. Scanning probe microscopy based nanoscale patterning and fabiraction. Selected Topics in Nanoscience and Nanotechnology 2007;3:1-21.

[5] Trybula WJ. Status of 157 nm optical lithography. J Microlithography Microfabrication Microsystems 2005;4:11007-11.

[6] Austin MD, Ge H, Wu W, Li M, Yu Z, Wasserman D, Lyon, SA, Chou SY. Fabrication of 5 nm linewidth and 14 nm pitch features by nanoimprint lithography. Appl Phys Lett 2004;84:5299–301.

[7] Olbrich A, Ebersberger B, Boit C, Niedermann P, Hänni,W, Vancea J, Hoffmann H. High aspect ratio all diamond tips formed by focused ion beam for conducting atomic force microscopy. J.Vac Sci Technol B 1999;17:1570-574

[8] Madou MJ. Fundamentals of Microfabrication: The science of Miniaturization, CRC press, New York. 2002.

[9] Park YD, Jung KB, Overberg M, Temple D, Pearton SJ, Holloway PH. Comparative study of Ni nanowires patterned by electron-beam lithography and fabricated by lift-off and dry etching techniques. J Vac Sci Technol B 2000;18:16-20.

[10] Xia Y, Whitesides GM. Soft lithography. Ann Rev Mater Sci 1998;28:153–84.

[11] Aizenberg J, Black AJ, Whitesides GM. Controlling local disorder in selfassembled monolayers by patterning the topography of their metallic supports. Nature 1998;394:868–71.

[12] Ostendorf A, Kamlage G, Chichkov BN. Precise deep drilling of metals by femtosecond laser pulses, RIKEN Review No. 50 (January, 2003): Focused on Laser Precision Microfabrication (LPM 2002).

[13] Quate CF. Scanning probes as a lithography tool for nanostructures. Surf Sci 1997;386:259–64.

[14] Malshe AP, Virwani KR, Rajurkar KP. Deshpande D. Investigation of nanoscale electro machining (nano-EM) in dielectric oil. Ann CIRP – Manuf Technol 2005;54:175-78.

[15] Virwani KR, Malshe AP, Rajurkar KP. Understanding Dielectric Breakdown and Related Tool Wear Characteristics in Nanoscale Electro-Machining Process. Ann CIRP – Manuf Technol 2007:56:217-20.

[16] Kalyanasundaram V, Virwani KR, Spearot DE, Rajurkar KP, Malshe AP. Understanding Repeatability in Nanoscale Electro-Machining Process. Transactions of NAMRI/SME 2008,36:145–52.

[17] Malshe AP, Rajurkar KP, Virwani KR, Taylor C, Bourell D, Levy G, Sundaram MM, Kalyanasundaram V, Samant A. Tip Based Nanomanufacturing using Electrical, Chemical, Mechanical and Thermal Processes. Ann CIRP – Manuf Technol 2010;59:628-51.

[18] Xie XN, Chung HJ, Sow CH, Wee ATS. Nanoscale materials patterning and engineering by atomic force microscopy nanolithography. Mater Sci Eng R 2006;54:1–48.

[19] Binnig G, Rohrer H, Gerber H, Weibel E. Surface studies by scanning tunneling microscopy. Phys Rev Lett 1982;49:57–61.

[20] Stroscio JA. Atomic and molecular manipulation with the scanning tunneling microscope, Science 1991;254:319-26.

[21] Hansen O, Ravnkilde JT, Quaade U, Stokbro K, Grey F. Field-induced deformation as a mechanism for scanning tunneling microscopy based nanofabrication, Phys Rev Lett 1998;81:5572-575.

[22] Chi Q, Zhang JD, Friis EP, Andersen JET, Ulstrup J. Creating nanoscale pits on solid surfaces in aqueous environment with scanning tunnelling microscopy. Surface Science 2000;463:L641–L648.

[23] Jahan MP, Rajurkar KP, Malshe AP. Experimental Investigation and Characterization of Nano-Scale Dry Electro-Machining. J Manuf Process 2012;14:443–51.

[24] Virwani KR, Malshe AP, Rajurkar KP. Understanding Dielectric Breakdown and Related Tool Wear Characteristics in Nanoscale Electro-Machining Process. CIRP Ann - Manuf Technol 2007;56:217–20.

[25] Kalyanasundaram V, Spearot DE, Malshe AP. Molecular Dynamics Simulation of Nanoconfinement Induced Organization of n-Decane. Langmuir 2009;25:7553–560.

[26] Brar VW, Zhang Y, Yayon Y, Ohta T, McChesney JL, Bostwick A, Rotenberg E, Horn K, Crommie MF. Scanning tunneling spectroscopy of inhomogeneous electronic structure in monolayer and bilayer graphene on SiC. Appl Phys Lett 2007;91:122102.

[27] Dimiev A, Kosynkin DV, Sinitskii A, Slesarev A, Sun Z, Tour JM. Layer-by-layer removal of graphene for device patterning. Science 2011;331:1168-172.

[28] Fox D, O'Neill A, Zhou D, Boese M, Coleman JN, Zhang HZ. Nitrogen assisted etching of graphene layers in a scanning electron microscope. Appl Phys Lett 2011;98:243117.

[29] Lee GD, Wang CZ, Yoon E, Hwang NM, Ho KM. Reconstruction and evaporation at graphene nanoribbon edges, Phys Rev B 2010:81:195419.

[30] Shenoy VB, Reddy CD, Zhang, YW. Spontaneous Curling of Graphene Sheets with Reconstructed Edges. ACS Nano 2010;4:4840-844.

[31] Virwani KR, Malshe AP, Rajurkar KP. Understanding Sub-20 nm Breakdown Behavior of Liquid Dielectrics. Phys Rev Lett 2007;99:017601.